Reassessment of long-period constituents for tidal predictions along the German North Sea coast and its tidally influenced rivers

Andreas Boesch[1] and Sylvin Müller-Navarra[1]

[1]Bundesamt für Seeschifffahrt und Hydrographie, Bernhard-Nocht-Straße 78, 20359 Hamburg, Germany

Correspondence: Andreas Boesch (andreas.boesch@bsh.de)

Abstract. The Harmonic Representation of Inequalities is a method for tidal analysis and prediction. With this technique, the deviations of heights and lunitidal intervals, especially of high and low waters, from their respective mean values are represented by superpositions of long-period tidal constituents. This study documents the preparation of a constituents list for the operational application of the Harmonic Representation of Inequalities. Frequency analyses of observed heights and

5   lunitidal intervals of high and low water from 111 tide gauges along the German North Sea coast and its tidally influenced rivers have been carried out using the generalized Lomb-Scargle periodogram. One comprehensive list of partial tides is realized by combining the separate frequency analyses and by applying subsequent improvements, e.g. through manual inspections of long-time data. The new set of 39 partial tides largely confirms the previously used set with 43 partial tides. Nine constituents are added and 13 partial tides, mostly in close neighbourhood of strong spectral components, are removed. The effect of these

10   changes has been studied by comparing predictions with observations from 98 tide gauges. Using the new set of constituents, the standard deviations of the residuals are reduced by 2.41% (times) and 2.30% (heights) for the year 2016. The new set of constituents is used for tidal analyses and predictions starting with the German tide tables for the year 2020.

1 Introduction

Tidal predictions for the German Bight are calculated at the Federal Maritime and Hydrographic Agency (*Bundesamt für*

15   *Seeschifffahrt und Hydrographie*, BSH) and are published in official tide tables each year. The preparation of tidal predictions has a long tradition at BSH and its predecessor institutions: the first tide tables by the German Imperial Admiralty were issued for the year 1879.

Since 1954, a method named Harmonic Representation of Inequalities (HRoI) is used at BSH to calculate tidal predictions for tide gauge locations along the German North Sea coast and its tidally influenced rivers (Horn, 1948, 1960; Müller-Navarra,

20   2013). This technique allows analysing the deviations of times and heights, especially at high and low water, from their respective mean values. In contrast to the widely used harmonic method, the HRoI utilizes only long-period partial tides. This reduction in frequency space allows for a computationally efficient way to calculate times and heights of high and low water. The HRoI has proven to be especially useful for predicting semi-diurnal tides in shallow waters where the harmonic method would need a large number ($\gtrsim 60$) of constituents or could even fail to produce adequate results. The fundamentals of the HRoI

25   are summarized in Sect. 2 for completeness.

An important aspect of tidal prediction is the selection of relevant partial tides (angular velocities) to be included in the underlying analysis of water level records. While it is possible to determine these partial tides individually for each single tidal analysis, it is desirable in an operational service to have one comprehensive set of constituents that can be used for all tide gauges under investigation. Horn (1960) presented a list of 44 angular velocities that were used with the HRoI. This selection

5   of partial tides was probably utilized until the year 1969 when the set was slightly modified (compare Tab. 2 in Sect. 2). To our knowledge, no documentation exists of the methods and specific water level records that were used to prepare these lists of angular velocities.

The objective of this work is to review the set of partial tides used with the HRoI by determining the most important long-period constituents for applications in the German Bight. Therefore, we perform a spectral analysis of water level observations

10   from 111 tide gauges. The available tide gauge data is presented in Sect. 3. The analysis of high and low water time series is described in Sect. 4. In Sect. 5, tidal predictions based on an existing list of partial tides and predictions based on the new set are compared with observed water levels.

2   Harmonic Representation of Inequalities

The Harmonic Representation of Inequalities (HRoI) is a derivative of the non-harmonic method by essentially translating it

15   into an analytical form. The non-harmonic method has been used for a long time, e.g. by Lubbock (1831) for the analysis of tides in the port of London. With the non-harmonic method, the times of high and low water are calculated by adding mean lunitidal intervals and corresponding inequalities to the times of lunar transits. Likewise, the heights of high and low water are determined by adding corresponding inequalities to the respective mean heights. The inequalities are corrections for the relative positions of earth, moon and sun (e.g. semi-monthly, parallactic, declination).

20   The original implementation of the HRoI, as introduced by Horn (1948, 1960), can be used to calculate vertices of tide curves, i.e. high water time, high water height, low water time and low water height. In this form the method is tailored to semi-diurnal tides. Müller-Navarra (2013) shows how the HRoI may be generalized to predict tidal heights at equidistant fractions of the mean lunar day. This generalization allows the determination of the full tidal curve at a chosen sampling interval. Here, we focus only on the application of calculating the times and heights of high and low water.

25   Let $(t_j, h_j), j = 1, ..., J$, be a time series of length J of high and low water heights h_j recorded at times t_j. All times need to be given in UTC. The HRoI method is based on the assumption that the variations of the individual heights and lunitidal intervals around their respective mean values can be described by sums of harmonic functions. The lunitidal interval is the time difference between the time t_j and the corresponding lunar transit at Greenwich. As a general rule, the daily higher high water and the following low water are assigned to the previous upper transit, and the daily lower high water and the following low

30   water are assigned to the previous lower transit. For example, in the year 2018, the mean lunitidal interval for high (low) water was determined to be 9 h 4 min (16 h 5 min) for Borkum and 15 h 22 min (22 h 32 min) for Hamburg.

A convenient method to organize high and low waters of semi-diurnal tides is the lunar transit number n_t (Müller-Navarra, 2009). It counts the upper lunar transits at the Greenwich meridian since the transit on December 31, 1949, which has been

Table 1. The high and low waters are classified into four types (event index k).

k	description
1	high water assigned to upper transit
2	low water assigned to upper transit
3	high water assigned to lower transit
4	low water assigned to lower transit

arbitrarily set to $n_t = 0$. A lower transit always has the same transit number as the preceding upper transit. Each high and low water is uniquely identified by using the number n_t of the assigned lunar transit and an additional event index k as defined in Tab. 1. The differentiation between upper and lower transit allows for changes in the Moon's declination which alternately advance and retard times, and increase and decrease the heights of successive tides (diurnal inequality).

5   A tidal analysis with the HRoI comprises the investigation of eight times series (heights and lunitidal intervals of the four event types listed in Tab. 1). Each time series is described by a model function of the following form:

$$\hat{y}(n_t) = a_0 + \sum_{l=1}^{L} \left[a_l \cos(\omega_l n_t) + a_{l+L} \sin(\omega_l n_t) \right]. \tag{1}$$

The parameters $a_l, l = 0, ..., 2L$ are determined from a least-squares fit, i.e.

$$\chi^2 = \sum_{j=0}^{J} \left(y_j - \hat{y}_j \right)^2 \rightarrow \min \quad , \tag{2}$$

10   where y_j are the observed heights or lunitidal intervals. The angular velocities ω_l are taken from a previously defined set of L partial tides. In Tab. 2, we list two sets of partial tides that have been used in the past at BSH and the new set that is the result of this work.

Table 2. Sets of angular velocities that have been used with the HRoI. See Sect. 2 for a description of the columns.

Doodson	m_s	m_h	m_p	$m_{N'}$	ω [°/h]	ω [°/tn]	name	set 1[a]	set 2[b]	this work
ZZZZAZ	0	0	0	1	0.0022064	0.0548098		x	x	x
ZZZAZZ	0	0	1	0	0.0046418	0.1153082			x	
ZZZBZZ	0	0	2	0	0.0092836	0.2306165				x
ZZAYZZ	0	1	-1	0	0.0364268	0.9048862			x	
ZZAZZZ	0	1	0	0	0.0410686	1.0201944	Sa	x	x	x
ZZBXZZ	0	2	-2	0	0.0728537	1.8097724		x	x	x
ZZBZZZ	0	2	0	0	0.0821373	2.0403886	Ssa	x	x	x
ZAXZZZ	1	-2	0	0	0.4668792	11.5978420		x	x	x
ZAXAZZ	1	-2	1	0	0.4715211	11.7131503	MSm	x	x	x
ZAYXZZ	1	-1	-2	0	0.4986643	12.3874200				x
ZAYZZZ	1	-1	0	0	0.5079479	12.6180365				x
ZAYAAZ	1	-1	1	1	0.5147961	12.7881545				x
ZAZYYZ	1	0	-1	-1	0.5421683	13.4681129		x	x	
ZAZYZZ	1	0	-1	0	0.5443747	13.5229227	Mm	x	x	x
ZAZZYZ	1	0	0	-1	0.5468101	13.5834211		x	x	
ZAZZZZ	1	0	0	0	0.5490165	13.6382309		x	x	x
ZAZZAZ	1	0	0	1	0.5512229	13.6930407		x	x	x
ZAZAZZ	1	0	1	0	0.5536583	13.7535391				x
ZABYZZ	1	2	-1	0	0.6265120	15.5633115		x	x	
ZABBAZ	1	2	2	1	0.6426438	15.9640460				x
ZBVBZZ	2	-4	2	0	0.9430421	23.4263005		x		
ZBWZZZ	2	-3	0	0	0.9748271	24.2158785		x	x	x
ZBXZYZ	2	-2	0	-1	1.0136894	25.1812631		x	x	x
ZBXZZZ	2	-2	0	0	1.0158958	25.2360729	MSf	x	x	x
ZBXZAZ	2	-2	0	1	1.0181022	25.2908827		x	x	
ZBXAZZ	2	-2	1	0	1.0205376	25.3513811		x	x	
ZBYZZZ	2	-1	0	0	1.0569644	26.2562673				x
ZBZXZZ	2	0	-2	0	1.0887494	27.0458453		x	x	x
ZBZYZZ	2	0	-1	0	1.0933912	27.1611535		x	x	x
ZBZZYZ	2	0	0	-1	1.0958266	27.2216520		x	x	
ZBZZZZ	2	0	0	0	1.0980330	27.2764618	Mf	x	x	x

Doodson	m_s	m_h	m_p	$m_{N'}$	ω [°/h]	ω [°/tn]	name	set 1[a]	set 2[b]	this work
ZBZZAZ	2	0	0	1	1.1002394	27.3312716		x	x	x
ZCVAZZ	3	-4	1	0	1.4874168	36.9492232	Sν2	x	x	x
ZCWYZZ	3	-3	-1	0	1.5192018	37.7388011		x	x	
ZCXYYZ	3	-2	-1	-1	1.5580641	38.7041858		x	x	
ZCXYZZ	3	-2	-1	0	1.5602705	38.7589956	SN	x	x	x
ZCXYAZ	3	-2	-1	1	1.5624769	38.8138054		x	x	
ZCXZZZ	3	-2	0	0	1.5649123	38.8743038		x	x	x
ZCXAZZ	3	-2	1	0	1.5695541	38.9896120	MStm	x	x	x
ZCZWZZ	3	0	-3	0	1.6331241	40.5687675		x		
ZCZYZZ	3	0	-1	0	1.6424077	40.7993844	Mfm	x	x	x
ZDUZZZ	4	-5	0	0	1.9907229	49.4519514		x	x	x
ZDVZZZ	4	-4	0	0	2.0317915	50.4721458	2SM	x	x	x
ZDXXZZ	4	-2	-2	0	2.1046452	52.2819182		x	x	
ZDXZZZ	4	-2	0	0	2.1139288	52.5125347	MSqm	x	x	x
ZDXZAZ	4	-2	0	1	2.1161352	52.5673444				x
ZDZZZZ	4	0	0	0	2.1960661	54.5529235		x	x	x
ZETAZZ	5	-6	1	0	2.5033126	62.1852961		x	x	x
ZEVYZZ	5	-4	-1	0	2.5761662	63.9950685	2SMN	x	x	x
ZEVZZZ	5	-4	0	0	2.5808080	64.1103767		x		
ZEVAZZ	5	-1	1	0	2.5854499	64.2256849				x
ZEXYZZ	5	-2	-1	0	2.6583035	66.0354573		x	x	
ZFTZZZ	6	-6	0	0	3.0476873	75.7082187		x	x	x
ZFVZZZ	6	-4	0	0	3.1298246	77.7486076		x	x	x
ZHRZZZ	8	-8	0	0	4.0635830	100.9442917		x	x	x
Number of partial tides in set of constituents:								44	43	39

[a] set 1 was probably used until the year 1969, see also Tab. 3 in Horn (1960). [b] set 2 was probably used from 1970

until 2019, see also appendix E in Goffinet (2000), Tab. 5 in Müller-Navarra (2013) includes $\omega = 23.4263005°/\text{tn}$

but this angular velocity has never been included in calculations for BSH tide tables or tide calendars.

All tidal constituents considered here have angular velocities that are linear combinations of the rate of change of four

fundamental astronomical variables: the mean longitude of the moon (s), the mean longitude of the sun (h), the mean longitude

of the lunar perigee (p) and the negative of the longitude of the moon's ascending node (N'). The second to fifth column in

5 Tab. 2 give the respective linear coefficients m. The coefficients for the rate of change of the mean lunar time and of the mean

longitude of the solar perigee are always equal to zero, because only long-period times are considered and the time series are

too short to resolve differences due to the variations of the solar perigee. The angular velocities in the sixth and seventh column

are given in degrees per hour and in degrees per transit number (unit symbol: tn), respectively. They are calculated using the

expressions for the fundamental arguments as published by the International Earth Rotation and Reference Systems Service (2010, Sect. 5.7). The first column is the alphabetical Doodson number and the eighth column states the commonly used names. A mark in one of the last three columns indicates whether the angular velocity is included in the respective constituents list for usage with the HRoI.

5   According to Horn (1960), the HRoI combines the best from the harmonic and the non-harmonic method: the analytical procedure of the first method, and the principle of calculating isolated values directly which is characteristic for the second. The strength of the HRoI lies in the prediction of times and heights of high and low water when the full tidal curve is considerably non-sinusoidal. This is frequently the case in shallow waters and rivers.

3   Tide gauge data

10   The tide gauges at the German coast and rivers are operated by different federal and state authorities. These agencies provide BSH with quality checked water level records of high and low waters (times and heights). Table A1 in the appendix lists 137 German tide gauges which deliver water level observations on a regular basis and for which tidal predictions were published in BSH tide tables (*Gezeitentafeln*) or tide calendar (*Gezeitenkalender*) for the year 2018 (Bundesamt für Seeschifffahrt und Hydrographie, 2017a, b). For the analysis presented in Sect. 4, all data until the year 2015 is considered that was systematically

15   archived in electronic form at BSH tidal information service (as of August 2018). The data periods are given in the fourth and fifth column in Tab. A1 and cover $22-27$ years for most gauges. Much longer time series are available for tide gauges Cuxhaven (BSH gauge number DE__506P) and Hamburg (DE__508P) for which data since the year 1901 is used. We are aware that the tidal regime can change over such a long time, but include all available data in the analysis to maximize the achievable spectral resolution.

20   Only tide gauges with more than 19 years of data are included in order to cover the period of rotation of the lunar node (18.6 years) in the frequency analysis. In addition, we use only tide gauges where more than 60% of high and low waters are recorded during the gauge's data period. This criterion excludes gauges for which no low water observations are available. The 111 gauges that fulfill these two criteria are marked in the column labelled "used for analysis" in Tab. A1. The locations of the tide gauges are shown on the map in Fig. 1.

4   Analysis of high water and low water time series

25   The following analysis is applied to the water level records of all 111 tide gauges that are marked in the seventh column of Tab. A1 in the appendix.
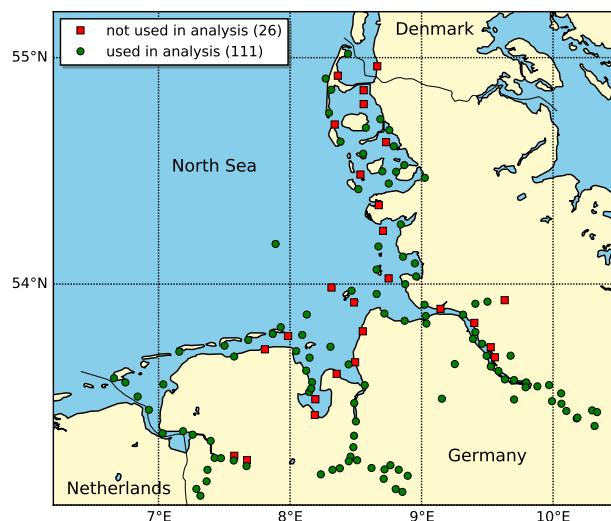
Figure 1. Locations of tide gauges from Table A1 in the German Bight.

4.1 Data preparation

Data preparation includes the assignment of lunar transit numbers and the calculation of lunitidal intervals as described in Sect. 2 for each record of high or low water. The lunar transit times are calculated using the algorithm by Meeus (1998) and the lunar coordinates from Chapront-Touzé and Chapront (1991).

5   The observed water levels include extreme events, such as storm surges. These events are not representative for the tidal behaviour at the site of a tide gauge and need to be removed from the data set. We apply a 3-sigma-clipping separately for the eight times series analysed with the HRoI (see Sect. 2). Only those data points are used in the analysis, for which the height and the lunitidal interval are within the range of three times the respective standard deviation.

4.2 Frequency analysis

10 The heights and lunitidal intervals are functions of the assigned transit number. We calculate periodograms for the heights and tidal intervals using the frequency scale tn^{-1}.

The tidal events are irregularly spaced in time. Additionally, there are many longer data gaps which cannot be interpolated. This excludes the fast Fourier transform (FFT) as spectral analysis technique. Instead, we use the generalized Lomb-Scargle periodogram as defined by Zechmeister and Kürster (2009), including their normalization if not mentioned otherwise. The

15 frequency scale covers the range from 0.000 1 to 2 tn^{-1} with an interval of 0.019 99 tn^{-1} (100 000 points in the periodogram). The upper limit corresponds to twice the sampling interval (Nyquist criterion).

Artefacts from spectral leakage pose a major problem when identifying peaks in a periodogram. They arise from the finite length of the time series (e.g. Press et al., 1992). This effect can be reduced by applying an appodization function that smoothly
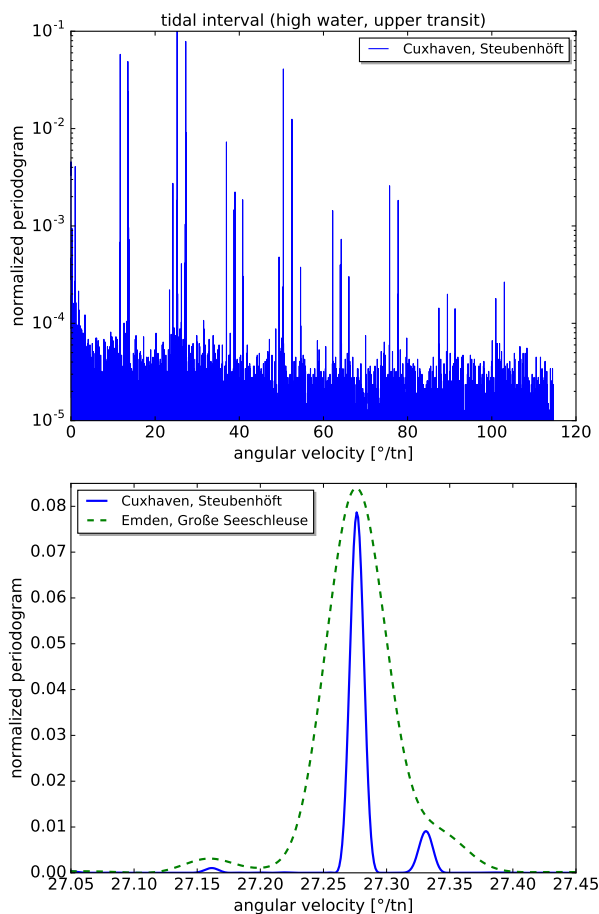
Figure 2. *Upper panel:* Normalized periodogram of the lunitidal intervals of high waters (assigned to upper lunar transits) for the tide gauge Cuxhaven. Notice the logarithmic scale which is truncated at 0.1 for better visibility of weak lines. *Lower panel:* Zoom into the region with the spectral line corresponding to half a tropical month (Mf) at 27.2764618°/tn. The longer time series for Cuxhaven leads to narrower spectral lines (solid blue curve) compared to Emden (dashed green line).

brings the recorded values to zero at the beginning and the end of the sampled time series. We apply a Hanning window to the data which gives a good compromise between reducing side lobes and preserving the spectral resolution.

For each tide gauge, periodograms are calculated for the eight time series that are analysed with the HRoI. In the upper panels of Fig. 2 and 3, we show periodograms of the lunitidal intervals and heights (of high waters assigned to an upper transit, $k = 1$) for the tide gauge Cuxhaven. Cuxhaven (together with Hamburg) provides by far the longest times series that is used in the analysis (compare Tab. A1). In these figures, the vertical axis is normalized to the strongest peak and the horizontal axis is converted to degrees per transit number for better comparison with Tab. 2. The periodogram for the lunitidal intervals reveals many more strong spectral lines above the noise floor as compared to the periodogram for the heights. A frequency depended
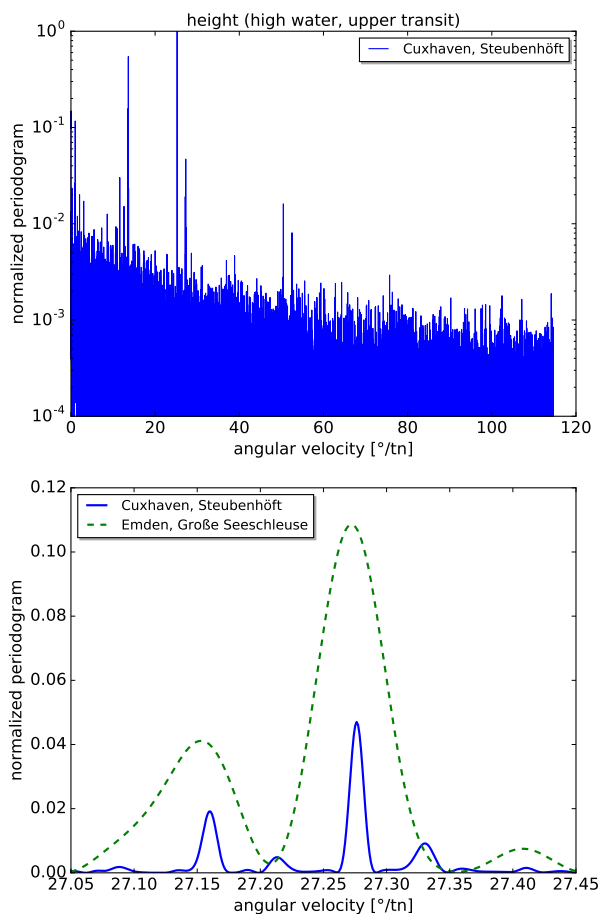
Figure 3. *Upper panel:* Normalized periodogram of the heights of high waters (assigned to upper lunar transits) for the tide gauge Cuxhaven. Notice the logarithmic scale. *Lower panel:* Zoom into the region with the spectral line corresponding to half a tropical month (Mf) at 27.2764618°/tn. The longer time series for Cuxhaven leads to narrower spectral lines (solid blue curve) compared to Emden (dashed green line).

noise level can clearly be seen in Fig. 3 (noise level increases towards lower angular velocities). The lower panels of Fig. 2 and 3 show a small extract of the respective upper periodograms. Additionally, data for tide gauge Emden is included for illustration of the differences in spectral line width. The time series from Emden is about four times shorter than the one from Cuxhaven. This leads to broader spectral lines in the periodogram and it can be expected that some weaker lines are unresolvable.

5 **4.3 Identifying relevant partial tides**

We aim to find all local maxima in a periodogram that are above a noise threshold. This threshold is calculated in a two-step process that is described in the following.
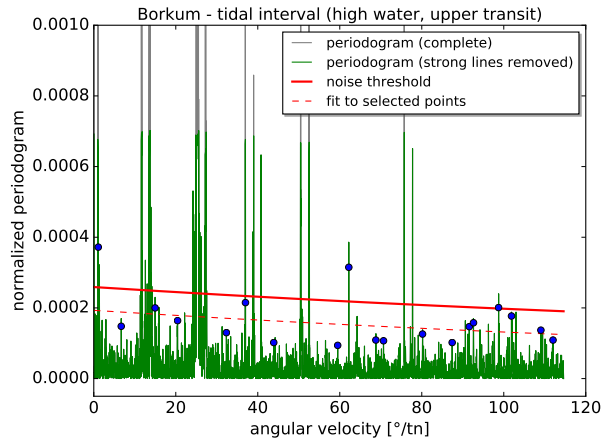
Figure 4. Determination of the noise threshold for the tidal interval (high water, upper transit) at tide gauge Borkum, Fischerbalje: the strongest lines are removed from the periodogram (grey vs. green lines) and an exponential function (dashed red curve) is fitted to selected points (blue). The noise threshold (thick red line) is shifted up by one standard deviation. See text for more details.

In the first step, the strongest spectral lines are removed from the periodogram. The values above the 99.5th percentile are removed from the data set and a histogram is calculated from the remaining values p (100 bins with central values x_{bin}). The histogram shows an exponential trend from a high number of data points with low periodogram values to a few points that fall into the bins at the upper end. An exponential curve $y_{bin} = a \cdot \exp(-x_{bin}/b)$ is fitted to the histogram, with fit parameters a and

5   b. The process of removing data points above the 99.5th percentile from the periodogram is repeated until the ratio $\max(p)/b$ falls below the value of 30. This value is based on experience.

In the second step, the noise threshold is determined using a set of remaining points in the periodogram that represent a continuum above the noise level. The result is illustrated in Figs. 4 and 5 for lunitidal intervals and heights at the tide gauge Borkum. For this procedure, the periodogram is split into 25 sections. The data point at the 99.5th percentile is selected in each

10   section and an exponential function is fitted to these 25 points. The fit is repeated after a 1-sigma-clipping. The noise threshold corresponds to the resulting exponential function plus one standard deviation (solid red line in Figs. 4 and 5).

The noise threshold functions from all tide gauges are averaged separately for lunitidal intervals, $L_i(\omega)$, and heights, $L_h(\omega)$:

$$L_i = 0.0004816 \cdot \exp(-0.0101045\,\text{tn}/^\circ \cdot \omega) \quad ,$$

$$L_h = 0.0024472 \cdot \exp(-0.0149899\,\text{tn}/^\circ \cdot \omega) \quad .$$

15   These two functions represent mean lower intensity boundaries for the selection of significant peaks.

A second selection criterion is the number of occurrences of the local maxima in the periodograms and their assignment to the partial tides having well known angular velocities. The angular velocities of 1268 potential partial tides have been precalculated. The ranges of the linear coefficients m for the fundamental variables are chosen based on experience:
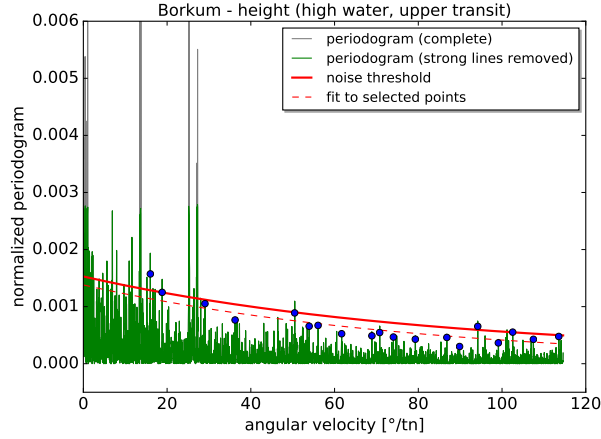
Figure 5. Same as Fig. 4 but for the heights at tide gauge Borkum, Fischerbalje.

$$m_s = 0, ..., 8$$

$$m_h = -8, ..., 3$$

$$m_p = -2, ..., 3, \quad \text{if } ((m_s = 0 \text{ and } m_h \geq 0)$$

$$\text{or } (m_s > 0 \text{ and } m_h \geq -m_s - 1))$$

5    $$m_{N'} = -1, 0, 1, \quad \text{if } ((m_s = 0 \text{ and } m_h = 0$$

$$\text{and } m_p = 0 \text{ and } m'_N \geq 0)$$

$$\text{or } (m_s \neq 0 \text{ or } m_h \neq 0$$

$$\text{or } m_p \neq 0))$$

A partial tide from the precalculated list is assigned uniquely to the closest peak in the periodogram if the difference in

10   angular velocity is less than half the spectral resolution. The spectral resolution r is defined as

$$r = 360°/T \quad , \tag{3}$$

with T being the length of the time series in transit numbers. For example, the spectral resolution of a time series of 19 years is

$$r = \frac{360°}{19\,\text{yr} \cdot 365.25\,\text{d/yr} \cdot \tau} = 0.05°/\text{tn} \quad , \tag{4}$$

where $\tau = 1.03505013\,\text{d/tn}$ is the length of the mean lunar day.

15   For each identified partial tide, we calculate (i) the percentage of periodograms in which the partial tide has been detected,

separately for lunitidal interval (N_i) and height (N_h); and (ii) the average intensity in the periodograms, separately for lunitidal

interval (I_i) and height (I_h). In order to be considered relevant, a partial tide with angular velocity ω must meet the following

criteria: $N_i \geq 33\%$ and $I_i(\omega) > L_i(\omega)$, or $N_h \geq 33\%$ and $I_h(\omega) > L_h(\omega)$. All partial tides that meet these selection criteria are

listed Tab. 3.

Table 3. The most important partial tides that were identified in the periodograms. See Sect. 4.3 for information on selection criteria and I_i, I_h, N_i and N_h.

Doodson	ω [°/tn]	I_i [-]	I_h [-]	N_i [%]	N_h [%]
ZZZZAZ	0.054810	0.0086	0.0102	78	45
ZZZBZZ	0.230616	0.0019	0.0085	29	47
ZZAXZZ	0.789578	0.0009	0.0088	16	34
ZZAZZZ	1.020194	0.0070	0.0367	85	84
ZZBZZZ	2.040389	0.0013	0.0068	26	56
ZAXZZZ	11.597842	0.0009	0.0034	69	35
ZAXAZZ	11.713150	0.0234	0.0024	100	10
ZAYXZZ	12.387420	0.0006	0.0031	2	65
ZAYZZZ	12.618036	0.0007	0.0042	34	21
ZAYAAZ	12.788154	0.0005	0.0031	1	45
ZAZYZZ	13.522923	0.0112	0.0119	99	90
ZAZZZZ	13.638231	0.0105	0.0297	97	87
ZAZAZZ	13.753539	0.0006	0.0016	63	2
ZABBAZ	15.964046	0.0010	0.0032	1	70
ZBWZZZ	24.215878	0.0029	0.0081	83	7
ZBXZZZ	25.236073	0.4550	0.0706	100	92
ZBYZZZ	26.256267	0.0034	0.0079	55	9
ZBZYZZ	27.161154	0.0008	0.0021	43	29
ZBZZZZ	27.276462	0.0382	0.0070	100	85
ZCVAZZ	36.949223	0.0037	0.0013	99	25
ZCXYZZ	38.758996	0.0009	0.0014	89	9
ZCXAZZ	38.989612	0.0010	0.0004	96	0
ZCZYZZ	40.799384	0.0008	0.0000	93	0
ZDUZZZ	49.451951	0.0004	0.0000	38	0
ZDVZZZ	50.472146	0.0196	0.0025	100	73
ZDXZZZ	52.512535	0.0059	0.0015	99	15
ZDZZZZ	54.552924	0.0003	0.0003	43	0
ZETAZZ	62.185296	0.0006	0.0000	93	0
					continued on next page

continued from previous page					
Doodson	ω [°/tn]	I_i [-]	I_h [-]	N_i [%]	N_h [%]
ZEVYZZ	63.995068	0.0003	0.0001	61	0
ZEVAZZ	64.225685	0.0004	0.0000	78	0
ZFTZZZ	75.708219	0.0014	0.0003	98	2
ZFVZZZ	77.748608	0.0010	0.0003	97	5
ZHRZZZ	100.944292	0.0002	0.0000	36	0
ZHTZZZ	102.984681	0.0002	0.0002	37	0

4.4 Adjustment of constituent list and ranking

In this section, we describe adjustments made to the list of partial tides based on manual inspections of certain periodograms and other considerations for an operational application. These adjustments lead to the set of partial tides in Tab. 4.

5   The periodograms calculated from longer time series offer a higher spectral resolution and contain more spectral information compared to the periodograms of shorter time series. For example, this can be seen in the lower panels of Fig. 2 and 3 with periodograms based on time series from tide gauge Cuxhaven (115 years) and Emden (27 years). The higher information content from longer water level records needs to be appreciated and incorporated adequately. Therefore, the periodograms of Cuxhaven and Hamburg have been inspected manually to find partial tides that appear in the data of these two tide gauges and

10   might not be detectable in other periodograms. Six partial tides with the following Doodson numbers were identified and added to the list: ZAZZAZ (ZAZZZZ), ZBXZYZ (ZBXZZZ), ZBZXZZ, ZBZZAZ (ZBZZZZ), ZCXZZZ and ZDXZAZ (ZDXZZZ). The Doodson numbers in parenthesis are partial tides from Tab. 3 that differ only by $\Delta m_{N'} = \pm 1$. For these pairs, long time series are needed to clearly see two separate spectral lines in the periodograms.

The noise in the periodograms increases towards lower angular velocities and the identification of partial tides below $1°$/tn

15   becomes less clear. For this reason, and after inspecting several periodograms manually, the partial tide ZZAXZZ is considered to be a misidentification and has been removed from the list. The other way round, the partial tide ZZBXZZ has been added to the list, because of its importance for tide gauges located upstream in the Elbe river. Finally, we decided to cut the list after the eighth synodic month to keep the range of angular velocities consistent with previously used lists of partial tides (compare Tab. 2).

20   The final set of long-term partial tides from our analysis is listed in Tab. 4. In the last column, each partial tide is assigned a number R indicating its overall importance (in decreasing order). The rank R is calculated by the following procedure:

$$R_i = \text{rank}(\text{norm}(I_i(\omega) - L_i(\omega)) \cdot N_i)$$
$$R_h = \text{rank}(\text{norm}(I_h(\omega) - L_h(\omega)) \cdot N_h)$$
$$R = \text{rank}((3R_i + R_h)/4) \tag{5}$$

where the function norm() returns normalized values in the range [0,1] and the function rank() returns the position of a list element, if the list were sorted in increasing order. In Eq. 5, the results from lunitidal intervals are weighted higher because the noise level is lower in the respective periodograms.

Table 4. The modified and adopted new list of long-term partial tides. The rank R indicates the importance of a partial tide for tidal analysis.

Doodson	ω [°/tn]	description / name	rank R
ZZZZAZ	0.054810	lunar nodal precession	6
ZZZBZZ	0.230616	half lunar apsidal precession	13
ZZAZZZ	1.020194	tropical year / Sa	7
ZZBXZZ	1.809772		31
ZZBZZZ	2.040389	half tropical year / Ssa	17
ZAXZZZ	11.597842		14
ZAXAZZ	11.713150	MSm	8
ZAYXZZ	12.387420		34
ZAYZZZ	12.618036		19
ZAYAAZ	12.788154		39
ZAZYZZ	13.522923	anomalistic month / Mm	3
ZAZZZZ	13.638231	tropical month	4
ZAZZAZ	13.693041		38
ZAZAZZ	13.753539		21
ZABBAZ	15.964046		36
ZBWZZZ	24.215878		11
ZBXZYZ	25.181263		35
ZBXZZZ	25.236073	half synodic month / MSf	1
ZBYZZZ	26.256267		12
ZBZXZZ	27.045845		33
ZBZYZZ	27.161154		15
ZBZZZZ	27.276462	half tropical month / Mf	2
ZBZZAZ	27.331272		27
ZCVAZZ	36.949223	Sν2	10
ZCXYZZ	38.758996	SN	16
ZCXZZZ	38.874304		24
ZCXAZZ	38.989612	MStm	22
ZCZYZZ	40.799384	Mfm	23
ZDUZZZ	49.451951		29
ZDVZZZ	50.472146	fourth synodic month / 2SM	5
ZDXZZZ	52.512535	MSqm	9
		continued on next page	

continued from previous page			
Doodson	ω [°/tn]	description / name	rank R
ZDXZAZ	52.567344		37
ZDZZZZ	54.552924		30
ZETAZZ	62.185296		25
ZEVYZZ	63.995068	2SMN	28
ZEVAZZ	64.225685		26
ZFTZZZ	75.708219	sixth synodic month	20
ZFVZZZ	77.748608		18
ZHRZZZ	100.944292	eighth synodic month	32

The rank R can be used to select a sublist of partial tides when performing a tidal analysis of water levels with less than 18.6 years of data. This is important, because not all partial tides can be resolved against each other for shorter time series. The minimum difference in angular velocity is given by the resolution criterion (Eq. 3). Fig. 6 illustrates the resolvable partial tides

5   as a function of the length of the data record. Note that the high-ranked partial tide representing the tropical month ($R = 4$) cannot be included for time series shorter than about nine years. For tidal analysis of time series shorter than nine years, it is therefore often better to perform a reference analysis: 19 years of data are used from a different tide gauge with a similar tidal behaviour (e.g. similar course of the semi-monthly inequality) and the results are translated to the original gauge by applying the respective differences of the mean lunitidal intervals and mean heights. This way, nodal corrections can be avoided which

10   come with their own assumptions and approximations (e.g. Godin, 1986).
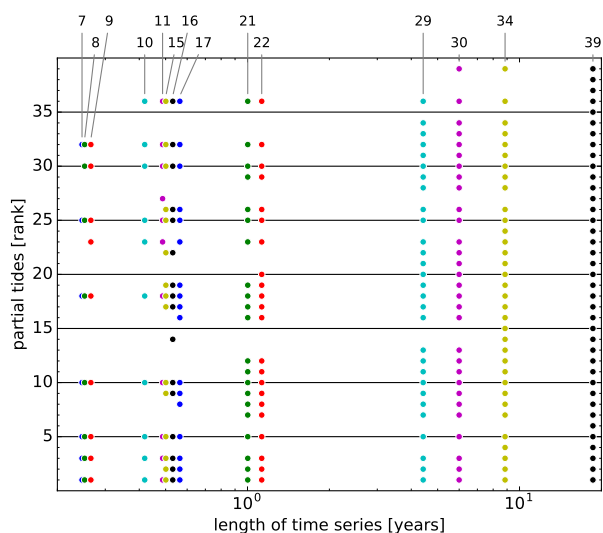
Figure 6. The partial tides (identified by their rank from Tab. 4) that can be resolved as a function of the (minimum) length of the time series. If two partial tides cannot be resolved against each other, the one with the lower rank is dropped. Note the logarithmic time axis from 0.2 to 20 years. The numbers at the top are the counts of partial tides.

5 Comparison of predictions with observations

For verification of the new constituent list, tidal predictions (i) based on an existing list of partial tides and (ii) based on the new set are compared with observations. The predictions are made for the year 2016 and are compared with tide gauge observations from the same year.

5.1 Tidal analysis and prediction

We calculate tidal predictions (time and height of high and low water) with the HRoI using (i) the 43 partial tides from "set 2" in Tab. 2 and (ii) the 39 partial tides derived from our analysis. The data and software are otherwise identical. The predictions are based on amplitudes a_m (see Eq. 1) that are determined from a tidal analysis of water level records from 1995 to 2013 (19 years). Only data from tide gauges are used that delivered enough observations in this time period to include all partial tides in the analysis. Additionally, the tide gauges must deliver observations for the year 2016. The 98 tide gauges that fulfill these criteria are marked in the column "used for verif." in Tab. A1. The tide gauge data is prepared and filtered as described in Sect. 4.1.

5.2 Evaluation of residuals

In Fig. 7, we show histograms of the residuals (observation−prediction) for the tide gauge Cuxhaven. The left and the right panel display histograms for the times and heights, respectively. Each panel contains one histogram for the tidal prediction with 43 partial tides (red) and one histogram for the tidal prediction with 39 partial tides (yellow). Using the new set of partial tides, the standard deviation of the residuals has decreased from 9.6 min to 9.0 min for the times and from 0.28 m to 0.27 m for the heights.
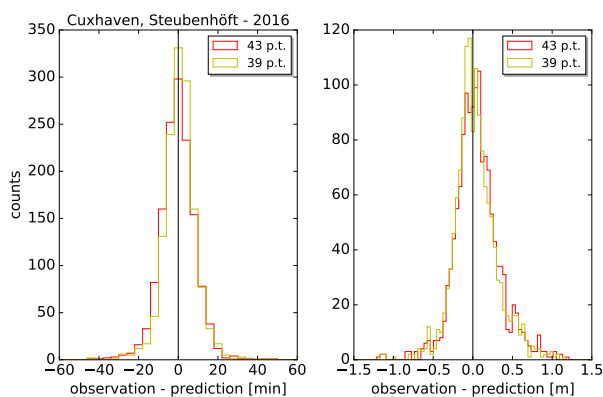
Figure 7. Histograms of the residuals for the two predictions based on different sets of partial tides for tide gauge Cuxhaven and year 2016. Left: time differences with a bin width of 4 min. Right: height differences with a bin width of 0.04 m.

Table 5. Residuals of predicted and observed times of high and low water: mean μ and standard deviation σ in minutes.

gauge number	gauge name	43 partial tides		39 partial tides	
		μ	σ	μ	σ
101P	Borkum	−2.7	11.2	−2.1	11.0
103P	Bremerhaven	−6.4	10.4	−4.6	10.1
111P	Norderney	1.5	10.9	0.7	10.6
502P	Bremen	−7.3	10.8	−5.5	10.5
505P	Büsum	3.4	17.5	4.6	17.4
506P	Cuxhaven	−0.1	9.6	1.0	9.0
507P	Emden	−9.2	13.8	−8.2	13.3
508P	Hamburg	−10.1	10.4	−7.7	10.3
509A	Helgoland	−2.4	7.8	−2.6	7.7
510P	Husum	−5.1	12.0	−4.3	11.7
512P	Wilhelmshaven	−3.2	10.0	−2.7	9.6

Table 6. Residuals of predicted and observed heights of high and low water: mean μ and standard deviation σ in meters.

gauge number	gauge name	43 partial tides		39 partial tides	
		μ	σ	μ	σ
101P	Borkum	0.05	0.24	0.03	0.24
103P	Bremerhaven	0.06	0.28	0.04	0.28
111P	Norderney	0.03	0.25	−0.01	0.24
502P	Bremen	0.01	0.27	−0.01	0.26
505P	Büsum	0.04	0.29	0.01	0.28
506P	Cuxhaven	0.05	0.28	0.04	0.27
507P	Emden	−0.01	0.28	−0.02	0.27
508P	Hamburg	−0.08	0.33	−0.12	0.31
509A	Helgoland	0.03	0.25	0.02	0.24
510P	Husum	0.02	0.29	0.00	0.28
512P	Wilhelmshaven	0.05	0.27	0.03	0.27

The mean values μ and standard deviations σ of the residuals for eleven major ports are presented in Tab. 5 for the times and in Tab. 6 for the heights. Based on the results from all tide gauges, the average standard deviation of the residuals is 13.2 min or 0.28 m, respectively. In most cases, the new set of tidal constituents gives small improvements in μ and σ.

The percentage changes of the standard deviations for all 98 tide gauges are presented in Fig. 8 for the times and in Fig. 9
5   for the heights. The average reductions of the standard deviations in the residuals are 2.41% (times) and 2.30% (heights).
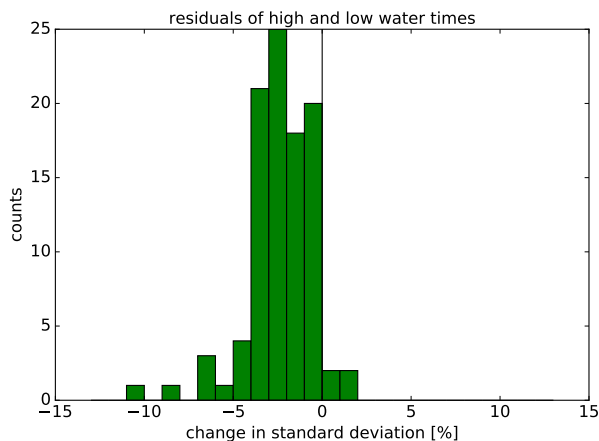
Figure 8. Histogram of the change in the standard deviation of the residuals of high and low water times for all 98 tide gauges.
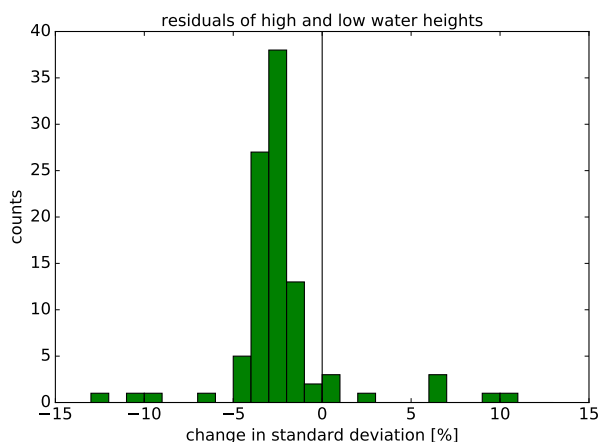
Figure 9. Histogram of the change in the standard deviation of the residuals of high and low water heights for all 98 tide gauges.

The change of constituents has an influence of the remaining periodicities in the residua. Periodograms are calculated for the two residua (times and heights) for each tide gauge. The 98 periodograms of each type are averaged. The resulting mean periodograms are shown in Fig. 10 and 11. In both figures, the strongest peaks are located at very low angular velocities ($\lesssim 1°$/tn). As mentioned before, the unambiguous identification of partial tides at these periods is difficult and consequently no
5 considerable improvements are achieved in reducing the (average) residual periodicities in this range. Four further strong peaks are visible in both figures at about 15, 25, 52 and 64°/tn for the prediction with 43 partial tides. These peaks could clearly be reduced with the new predictions (39 partial tides).
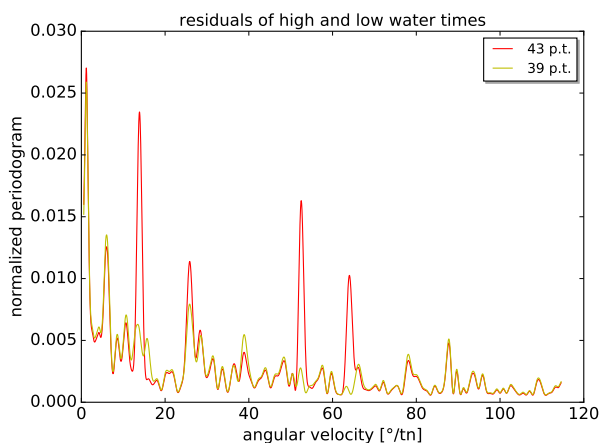
Figure 10. Mean periodogram of residual high or low water times for all tide gauges used in verification.
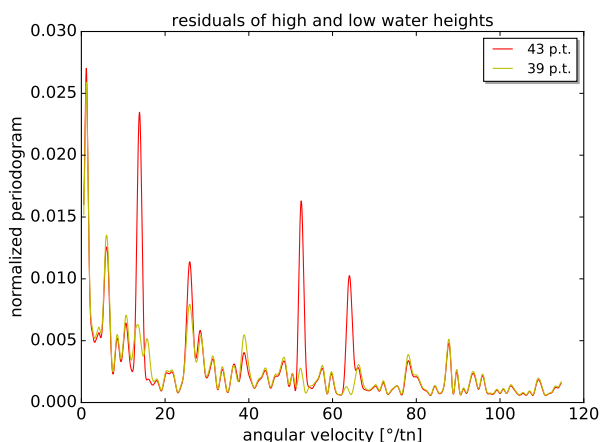
Figure 11. Mean periodogram of residual high or low water heights for all tide gauges used in verification.

6   Conclusions

Time series of high and low water from 111 German tide gauges were analysed to determine important long-period partial tides. An application is the usage of these constituents in tidal analyses and predictions with the HRoI. Generalized Lomb-Scargle periodograms were calculated for all tide gauges and spectral peaks were identified above noise thresholds. The separate

5   analyses of lunitidal intervals and heights were combined to realize one comprehensive list of partial tides for applications in the German Bight.

The new set of 39 partial tides largely confirms the previously used set with 43 partial tides. It can be seen from Tab. 2, that nine new constituents were added and 13 constituents were removed. Many of the removed angular velocities are close to

strong partial tides, such as the anomalistic month (Mm), the half synodic month (MSf) and the half tropical month (Mf). The removed constituents might have been artefacts from spectral leakage, which are most prominent in the proximity of strong spectral lines, that were misidentified as true signals in previous studies. The unambiguous identification of partial tides is very difficult at angular velocities below approximately 1°/tn because the noise levels in the periodograms increase towards lower

5   angular velocities and the results from different tide gauges are less consistent.

The verification based on observations from 98 tide gauges in the year 2016 suggests that the usage of the new constituents list leads to slightly better predictions. In particular, the average standard deviations of the residuals are lower and residual periodicities could be reduced around four frequencies.

This study presents for the first time a thorough investigations of the long-period constituents used with the HRoI. The new

10   list of constituents is used in tidal analyses and predictions with the HRoI for German tide gauges starting with the BSH tide tables for the year 2020.

Appendix A: Table of tide gauges

Table A1. 137 German tide gauges which deliver water level observations on a regular basis and for which tidal predictions were published in BSH tide tables (*Gezeitentafeln*) or tide calendar (*Gezeitenkalender*) for the year 2018. The data from the tide gauges are observed times and heights of high and low water. The tide gauges are operated by different federal and state agencies which provide tide gauge records to BSH. Abbreviations in the third column corresponds to the following agencies: E: Emden Waterways and Shipping Authority (Wasserstraßen- und Schifffahrtsamt Emden, WSA Emden), BH: WSA Bremerhaven, B: WSA Bremen, C: WSA Cuxhaven, T: WSA Tönning, HPA: Hamburg Port Authority, W: WSA Wilhelmshaven, HU: Landesbetrieb für Küstenschutz, Nationalpark und Meeresschutz Schleswig-Holstein (LKN-SH Husum), H: WSA Hamburg, L: WSA Lauenburg, N: Niedersächsischer Landesbetrieb für Wasserwirtschaft, Küsten- und Naturschutz (NLWKN), M: WSA Meppen.

BSH gauge number	gauge name	auth.	data period [start/end date]	data period [years]	completeness of data [%]	used for analysis	used for verif.
DE__101P	Borkum, Fischerbalje	E	02.01.1963-31.12.2015	53.0	62	x	x
DE__103P	Bremerhaven, Alter Leuchtturm	BH	01.11.1965-31.12.2015	50.2	62	x	x
DE__111P	Norderney, Riffgat	E	01.01.1964-31.12.2015	52.0	67	x	x
DE__502P	Bremen, Oslebshausen	B	01.01.1950-31.12.2015	66.0	99	x	x
DE__504A	Brunsbüttel, Mole 1	C	01.08.2010-31.12.2015	5.4	95		
DE__505P	Büsum	T	01.01.1963-31.12.2015	53.0	63	x	x
DE__506P	Cuxhaven, Steubenhöft	C	01.01.1901-31.12.2015	115.0	99	x	x
DE__507P	Emden, Große Seeschleuse	E	01.01.1989-31.12.2015	27.0	99	x	x
DE__508P	Hamburg, St. Pauli	HPA	01.01.1901-31.12.2015	115.0	100	x	x
DE__509A	Helgoland, Binnenhafen	T	01.01.1989-31.12.2015	27.0	99	x	x
DE__510P	Husum	T	01.01.1989-31.12.2015	27.0	98	x	x
DE__512P	Wilhelmshaven, Alter Vorhafen	W	01.01.1973-31.12.2015	43.0	98	x	x
DE__613C	Hojer, Schleuse	HU	01.01.1999-31.12.2015	17.0	100		
DE__617P	List, Hafen	T	01.01.1986-31.12.2015	30.0	98	x	x
DE__618P	Munkmarsch	HU	16.01.1989-31.12.2015	27.0	49		
DE__620P	Westerland	HU	01.01.1986-31.12.2015	30.0	94	x	x
DE__622P	Amrum Odde	HU	17.04.1996-07.12.2015	19.6	40		
DE__623A	Rantumdamm	HU	08.01.1996-31.12.2015	20.0	89	x	
DE__624P	Hörnum, Hafen	T	01.01.1989-31.12.2015	27.0	99	x	x
DE__628A	Osterley	HU	09.04.1997-11.11.2015	18.6	40		
DE__629B	Föhrer Ley Nord	HU	27.04.1994-11.11.2015	21.5	46		
DE__631P	Amrum, Hafen (Wittdün)	T	01.01.1989-31.12.2015	27.0	96	x	
DE__632P	Föhr, Wyk	HU	01.01.1989-31.12.2015	27.0	100	x	x

BSH gauge number	gauge name	auth.	data period [start/end date]	data period [years]	completeness of data [%]	used for analysis	used for verif.
DE__635P	Dagebüll	T	01.01.1989-31.12.2015	27.0	99	x	x
DE__636F	Hooge, Anleger	HU	01.01.1989-31.12.2015	27.0	93	x	x
DE__637A	Strand, Hamburger Hallig	HU	02.05.1989-31.12.2015	26.7	79	x	
DE__637P	Gröde, Anleger	HU	01.01.1989-31.12.2015	27.0	48		
DE__638P	Schlüttsiel	HU	01.01.1989-31.12.2015	27.0	96	x	x
DE__642C	Rummelloch, West	HU	14.06.1994-08.12.2015	21.5	47		
DE__645P	Süderoogsand	HU	23.03.1993-20.11.2015	22.7	62	x	
DE__647A	Pellworm, Anleger	T	01.03.1996-31.12.2015	19.8	88	x	
DE__649B	Holmer Siel	HU	01.01.1994-31.12.2015	22.0	89	x	x
DE__649P	Nordstrand, Strucklahnungshörn	HU	01.01.1989-31.12.2015	27.0	96	x	x
DE__653P	Südfall, Fahrwasserkante	HU	25.03.1993-02.12.2015	22.7	67	x	
DE__655D	Tümlauer Hafen	HU	24.09.2001-31.12.2013	12.3	93		
DE__658B	Linnenplate	HU	11.04.2001-05.12.2013	12.7	62		
DE__664P	Eidersperrwerk, AP	T	01.01.1989-31.12.2014	26.0	97	x	
DE__666P	Blauort	HU	12.01.1989-31.12.2015	27.0	82	x	x
DE__667B	Meldorf - Sperrwerk, AP	HU	04.01.1994-31.12.2015	22.0	71	x	
DE__669P	Deichsiel	HU	01.01.1989-31.12.2013	25.0	96	x	
DE__673P	Trischen, West	HU	18.03.1989-25.11.2015	26.7	61	x	
DE__675C	Mittelplate	HU	01.01.1992-25.11.2015	23.9	55		
DE__675P	Friedrichskoog, Hafen	HU	01.01.1989-31.12.2015	27.0	100	x	x
DE__676P	Zehnerloch	C	01.01.1989-14.11.2015	26.9	98	x	x
DE__677C	Scharhörnriff, Bake A	C	01.01.2001-31.12.2015	15.0	96		
DE__677P	Scharhörn, Bake C	C	01.01.1989-31.12.2015	27.0	98	x	x
DE__678W	Neuwerk	HPA	01.01.1994-31.12.2015	22.0	46		
DE__681A	Neufeld, Hafen	HU	01.01.1994-31.12.2015	22.0	78	x	x
DE__681P	Otterndorf	C	01.01.1989-31.12.2015	27.0	79	x	
DE__682P	Osteriff	C	01.01.1989-31.12.2015	27.0	89	x	
DE__683P	Belum, Oste	C	01.01.1989-31.12.2015	27.0	96	x	x
DE__685P	Hechthausen, Oste	C	01.01.1989-31.12.2015	27.0	95	x	x
DE__687P	Bremervörde, Oste	C	01.01.1989-31.12.2015	27.0	94	x	x
DE__688P	Brokdorf	H	01.01.1989-31.12.2015	27.0	98	x	x
DE__690P	Stör - Sperrwerk, AP	HU	01.01.2000-31.12.2015	16.0	87		
DE__691R	Kasenort, Stör	HU	01.01.1989-31.12.2015	27.0	99	x	x

BSH gauge number	gauge name	auth.	data period [start/end date]	data period [years]	completeness of data [%]	used for analysis	used for verif.
continued from previous page							
DE__692P	Itzehoe, Stör	H	01.01.1989-31.12.2015	27.0	97	x	
DE__693P	Breitenberg, Stör	H	01.01.2000-31.12.2015	16.0	95		
DE__695P	Glückstadt	H	01.01.1989-31.12.2015	27.0	95	x	x
DE__697P	Krautsand	H	01.01.1989-31.12.2015	27.0	89	x	x
DE__698P	Kollmar (Kamperreihe)	H	01.01.1989-31.12.2015	27.0	98	x	x
DE__700R	Krückau - Sperrwerk, BP	H	01.01.2000-31.12.2015	16.0	89		
DE__703P	Grauerort	H	01.01.1989-31.12.2015	27.0	98	x	x
DE__704R	Pinnau - Sperrwerk, BP	H	01.01.2000-31.12.2015	16.0	93		
DE__706P	Uetersen, Pinnau	H	01.01.1989-31.12.2015	27.0	92	x	x
DE__709P	Stadersand, Schwinge	H	01.01.1989-31.12.2015	27.0	98	x	x
DE__711P	Hetlingen	H	01.01.1989-31.12.2015	27.0	94	x	x
DE__712P	Lühort, Lühe	H	01.01.1989-31.12.2015	27.0	97	x	x
DE__714P	Schulau	H	01.01.1989-31.12.2015	27.0	97	x	x
DE__715P	Blankenese, Unterfeuer	HPA	01.01.1989-31.12.2015	27.0	98	x	x
DE__717P	Cranz, Este - Sperrwerk, AP	H	01.01.1989-31.12.2015	27.0	83	x	x
DE__718P	Buxtehude, Este	H	01.01.1989-31.12.2015	27.0	86	x	x
DE__720P	Seemannshöft	HPA	01.01.1989-31.12.2015	27.0	100	x	x
DE__724P	Harburg, Schleuse	HPA	01.01.1989-31.12.2015	27.0	100	x	x
DE__727P	Dove - Elbe, Einfahrt	HPA	01.01.1989-31.12.2015	27.0	99	x	x
DE__729P	Bunthaus	HPA	01.01.1989-31.12.2015	27.0	100	x	x
DE__730A	Ilmenau - Sperrwerk, AP	L	01.01.1989-31.12.2015	27.0	98	x	x
DE__730C	Fahrenholz, Ilmenau	L	01.01.1989-31.12.2015	27.0	93	x	x
DE__730P	Over	L	01.01.1989-31.12.2015	27.0	98	x	x
DE__731P	Zollenspieker	L	01.01.1989-31.12.2015	27.0	98	x	x
DE__732A	Altengamme	L	01.01.1989-31.12.2015	27.0	96	x	x
DE__732D	Geesthacht, Wehr UP	L	01.01.1989-31.12.2015	27.0	98	x	x
DE__734P	Alte Weser, Leuchtturm	BH	01.01.1989-31.12.2015	27.0	99	x	x
DE__735A	Spieka Neufeld	N	01.01.1989-31.12.2015	27.0	50		
DE__735B	Wremertief	N	01.01.1994-31.12.2015	22.0	38		
DE__737P	Dwarsgat, Unterfeuer	BH	01.01.1989-31.12.2015	27.0	99	x	x
DE__737S	Robbensüdsteert	BH	01.01.1989-31.12.2015	27.0	96	x	x
DE__738P	Fedderwardersiel	N	01.01.1989-31.12.2015	27.0	49		
DE__741A	Nordenham, Unterfeuer	BH	01.01.1989-31.12.2015	27.0	99	x	x

BSH gauge number	gauge name	auth.	data period [start/end date]	data period [years]	completeness of data [%]	used for analysis	used for verif.
DE__741B	Rechtenfleth	BH	01.01.1993-31.12.2015	23.0	99	x	x
DE__743P	Brake	B	01.01.1989-31.12.2015	27.0	97	x	x
DE__744A	Elsfleth Ohrt	B	01.01.1989-31.12.2015	27.0	96	x	x
DE__744P	Elsfleth	B	01.01.1975-31.12.2015	41.0	80	x	x
DE__745P	Huntebrück, Hunte	B	01.01.1989-31.12.2015	27.0	98	x	x
DE__746P	Hollersiel, Hunte	B	01.01.1989-31.12.2015	27.0	98	x	x
DE__747P	Reithörne, Hunte	B	01.01.1989-31.12.2015	27.0	98	x	x
DE__748P	Oldenburg - Drielake, Hunte	B	01.01.1989-31.12.2015	27.0	97	x	x
DE__749P	Farge	B	01.01.1989-31.12.2015	27.0	99	x	x
DE__750A	Wasserhorst, Lesum	B	01.01.1989-31.12.2015	27.0	90	x	x
DE__750B	Ritterhude, Hamme	B	01.01.1989-31.12.2015	27.0	91	x	x
DE__750C	Niederblockland, Wümme	B	01.01.1989-31.12.2015	27.0	91	x	x
DE__750D	Borgfeld, Wümme	B	01.01.1989-31.12.2015	27.0	90	x	x
DE__750P	Vegesack	B	01.01.1975-31.12.2015	41.0	80	x	x
DE__751P	Bremen, Wilhelm-Kaisen-Brück	B	01.01.1989-31.12.2015	27.0	99	x	x
DE__752P	Bremen, Weserwehr	B	01.01.1989-31.12.2015	27.0	98	x	x
DE__754P	Wangerooge, Langes Riff, (Nord)	W	01.01.1976-31.12.2015	40.0	71	x	x
DE__756P	Wangerooge, Ost	W	01.05.1976-31.12.2015	39.7	58		x
DE__760P	Mellumplate, Leuchtturm	W	01.01.1989-31.12.2015	27.0	99	x	x
DE__761P	Schillig	W	01.01.1989-31.12.2015	27.0	92	x	x
DE__764B	Hooksielplate	W	01.01.1989-31.12.2015	27.0	93	x	x
DE__766P	Voslapp	W	01.01.1989-31.12.2015	27.0	95	x	x
DE__769P	Wilhelmshaven, Ölpier	W	01.01.1989-31.12.2015	27.0	97	x	x
DE__770P	Wilhelmshaven, Neuer Vorhafen	W	01.01.1989-31.12.2015	27.0	97	x	x
DE__773P	Arngast, Leuchtturm	W	15.05.2001-31.12.2015	14.6	88		
DE__776P	Vareler Schleuse	N	01.01.1989-31.12.2015	27.0	49		
DE__777P	Wangerooge, West	W	01.01.1976-31.12.2015	40.0	73	x	x
DE__778P	Harlesiel	N	01.01.1989-31.12.2015	27.0	57		
DE__779P	Spiekeroog	E	01.01.1989-31.12.2015	27.0	98	x	x
DE__781P	Langeoog	E	01.01.1989-31.12.2015	27.0	98	x	x
DE__782P	Bensersiel	N	01.01.1989-31.12.2015	27.0	100	x	x
DE__796C	Leybucht, Leyhörn	N	01.01.1992-31.12.2015	24.0	100	x	x
DE__798P	Borkum, Südstrand	E	02.01.1989-31.12.2015	27.0	95	x	x

BSH gauge number	gauge name	auth.	data period [start/end date]	data period [years]	completeness of data [%]	used for analysis	used for verif.
				continued from previous page			
DE__799G	Dukegat	E	01.01.1989-31.12.2015	27.0	95	x	x
DE__799P	Emshörn	E	01.01.1989-31.12.2015	27.0	99	x	x
DE__802P	Knock	E	01.01.1989-31.12.2015	27.0	99	x	x
DE__803P	Pogum, Ems	E	01.01.1989-31.12.2015	27.0	98	x	x
DE__805P	Terborg, Meßstelle, Ems	E	01.01.1989-31.12.2015	27.0	98	x	x
DE__806P	Leerort, Ems	E	01.01.1989-31.12.2015	27.0	97	x	x
DE__808A	Leda - Sperrwerk, Unterpegel	E	01.01.1989-31.12.2015	27.0	98	x	x
DE__810A	Nortmoor, Altarm Jümme	N	01.01.2000-31.12.2015	16.0	85		
DE__810B	Detern, Jümme	N	01.01.2000-31.12.2015	16.0	86		
DE__810P	Westringaburg, Leda	N	01.01.1989-31.12.2015	27.0	84	x	x
DE__812P	Dreyschloot, Leda	E	01.01.1989-31.12.2015	27.0	89	x	x
DE__813P	Weener, Ems	E	01.01.1989-31.12.2015	27.0	98	x	x
DE__814B	Rhede, Ems	M	01.01.1989-31.12.2015	27.0	94	x	x
DE__814P	Papenburg, Ems	E	01.01.1989-31.12.2015	27.0	98	x	x
DE__816P	Herbrum, Hafendamm, Ems	M	01.01.1989-01.11.2015	26.8	82	x	
					Number of tide gauges	111	98

Competing interests. The authors declare that they have no conflict of interest.

References

Bundesamt für Seeschifffahrt und Hydrographie: Gezeitentafeln 2018. Europäische Gewässer, BSH, 2017a.

Bundesamt für Seeschifffahrt und Hydrographie: Gezeitenkalender 2018. Hoch- und Niedrigwasserzeiten für die Deutsche Bucht und deren Flussgebiete, BSH, 2017b.

5 Chapront-Touzé, M. and Chapront, J.: Lunar Tables and Programms from 4000 B.C. to A.D. 8000, Willmann-Bell, 1991.

Godin, G.: The use of nodal corrections in the calculation of harmonic constants, International Hydrographic Review, LXIII, 143–162, 1986.

Goffinet, P.: Qualitätssteigerung der Seevermessung und Navigation durch neuartige Beschickungsverfahren, Phd thesis, Universität Hannover, 2000.

Horn, W.: Über die Darstellung der Gezeiten als Funktion der Zeit, Deutsche Hydrographische Zeitschrift, 1, 124–140, 1948.

10 Horn, W.: Some recent approaches to tidal problems, International Hydrographic Review, 37, 65–84, 1960.

International Earth Rotation and Reference Systems Service: IERS Conventions (2010), Verlag des Bundesamts für Kartographie und Geodäsie, Frankfurt am Main, 2010.

Lubbock, J. W.: On the tides in the port of London, Philosophical Transactions of the Royal Society of London, 121, 349–415, https://doi.org/10.1098/rstl.1831.0022, 1831.

15 Meeus, J.: Astronomical Algorithms, Willmann-Bell, 1998.

Müller-Navarra, S.: Zur automatischen Scheitelpunktbestimmung gemessener Tidekurven in der Deutschen Bucht, Hydrologie und Wasserbewirtschaftung, 53, 380–388, 2009.

Müller-Navarra, S.: Gezeitenvorausberechnungen mit der Harmonischen Darstellung der Ungleichheiten (On Tidal Predictions by Means of Harmonic Representation of Inequalities), Berichte des Bundesamtes für Seeschifffahrt und Hydrographie, 50, 2013.

20 Press, W. H., Teukolsky, S. A., Vetterling, W. T., and Flannery, B. P.: Numerical Recipes in FORTRAN, Cambridge University Press, 1992.

Zechmeister, M. and Kürster, M.: The generalised Lomb-Scargle periodogram. A new formalism for the floating mean and Keplerian periodograms, A&A, 496, 577–584, https://doi.org/10.1051/0004-6361:200811296, 2009.